Radiation Protection Dosimetry (2005), Vol. 114, Nos 1-3, pp. 395–398
doi:10.1093/rpd/nch519

CALCULATION OF THE PROPERTIES OF DIGITAL MAMMOGRAMS USING A COMPUTER SIMULATION

R. A. Hunt[1], D. R. Dance[1,*], P. R. Bakic[2], A. D. A. Maidment[2], M. Sandborg[3], G. Ullman[3] and G. Alm Carlsson[3]
[1]Physics Department, The Royal Marsden NHS Foundation Trust, London SW3 6JJ, UK
[2]Department of Radiology, Hospital of the University of Pennsylvania, Philadelphia, PA 19104, USA
[3]Department of Radiation Physics, University of Linköping, SE-58185 Linköping, Sweden

A Monte Carlo computer model of mammography has been developed to study and optimise the performance of digital mammographic systems. The program uses high-resolution voxel phantoms to model the breast, which simulate the adipose and fibroglandular tissues, Cooper's ligaments, ducts and skin in three dimensions. The model calculates the dose to each tissue, and also the quantities such as energy imparted to image pixels, noise per image pixel and scatter-to-primary (S/P) ratios. It allows studies of the dependence of image properties on breast structure and on position within the image. The program has been calibrated by calculating and measuring the pixel values and noise for a digital mammographic system. The thicknesses of two components of this system were unknown, and were adjusted to obtain a good agreement between measurement and calculation. The utility of the program is demonstrated with the calculations of the variation of the S/P ratio with and without a grid, and of the image contrast across the image of a 50-mm-thick breast phantom.

INTRODUCTION

A Monte Carlo computer program has been developed to realistically model mammographic X-ray imaging systems. The model uses a voxelised phantom to simulate the breast; also the anatomical details can be included in the program and are used to estimate the measures of image quality. The program also calculates the doses to the different tissues simulated by the breast voxel phantom and in particular the mean glandular breast dose (MGD). When the MGD is calculated in combination with the measures of image quality, the model can be used for the optimisation of the mammographic imaging system.

This paper focuses on the use of program for studies of image properties. A calibration of the model by comparing the calculated and measured image properties for a digital mammographic unit is presented. The utility of the program is demonstrated with calculations of the variation of the scatter-to-primary (S/P) ratio with and without a grid, and of the image contrast for the visualisation of a small microcalcification, across the image of a 50-mm-thick breast phantom. Such detailed calculations have not been possible previously because of the lack of a suitable phantom to model the breast. A companion paper describes the use of the program for breast dosimetry[1].

*Corresponding author: david.dance@rmh.nthames.nhs.uk

METHODS

Monte Carlo model

The Monte Carlo computer program takes into account the mammographic X-ray spectrum, compression plate, breast support, anti-scatter grid and image receptor. It is based on the programs developed previously[2,3], which have been extended by the addition of a quasi-realistic voxel phantom that simulates the breast. The program follows photons from the focal spot of the X-ray tube, through the imaging system and the breast, simulating photoelectric interactions and coherent and incoherent scattering. All the energy deposited within each different breast tissue is recorded so that the dose to individual tissues and the mean glandular dose can be estimated. The program also calculates the energy imparted to the individual pixels from the primary and scattered photons. The sum of these is assumed to be proportional to the pixel value. The noise on these quantities is estimated by assuming that the only noise source is the variation in the energy deposited in the image receptor per photon (quantum mottle). The model can thus be used to study the variation of the S/P ratio and the signal-to-noise ratio (SNR) per pixel across the image. The S/P ratio has an important influence on the contrast obtained. The contrast itself is also calculated using the program by inserting a contrast detail in the phantom and calculating the image pixels with and without the details. The contrast-to-noise ratio for test details can be found in the same manner.

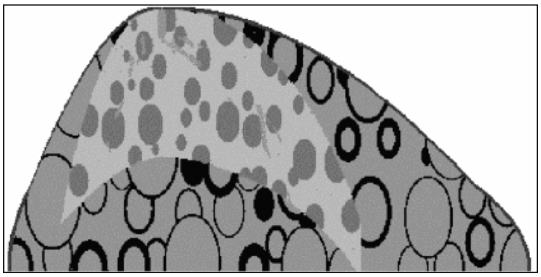

Figure 1. Cross section though the voxel phantom passing through the nipple and parallel to the image plane. The skin, 'surround' and central regions can be seen as well as the intersection of the ductal tree with the cross-sectional plane.

Voxel phantom

The anthropomorphic breast phantom used for this work was developed by Bakic *et al.*[4]. This phantom simulates the tissues within the breast in three dimensions. It consists of three regions: skin; a central region connected to the nipple, which contains adipose and fibroglandular tissues and a ductal tree; and a 'surround' region between the skin and central region, which contains adipose tissue and Cooper's ligaments. The voxel phantom was constructed in two stages. The uncompressed breast was modelled and the model breast was then compressed in the medial-lateral oblique projection and voxelised at 400 μm. A cross section of the anthropomorphic phantom in a plane through the nipple and parallel to the image is shown in Figure 1. Previous simple phantoms used by us to simulate the breast consisted of a truncated semi-cylinder of a mixture of glandular and adipose tissues surrounded by a uniform adipose 'shield' 5 mm thick on all the sides apart from the chest wall[2,3]. The phantom used for the present calculations corresponds to a 50-mm-thick compressed breast of 69% glandularity. (The term 'glandularity' refers to the fraction by weight of glandular and ductal tissues within the central region of the breast rather than the fraction by weight for the whole breast.) By using this phantom, values have been calculated for the S/P ratio with grid, S/P ratio without grid and the contrast of a 200 μm microcalcification on a 35×18 grid of points spanning the image, so that the variation and distribution of these quantities can be studied.

Calibration of the Monte Carlo simulation against experiment

The results of the Monte Carlo calculations of the energy deposited per pixel and the SNR per pixel were compared with the measurements on the images of sheets of polymethyl methacrylate (PMMA) obtained with a GE Senographe 2000D digital mammography unit. An Mo/Mo spectrum at 28 kV (half-value layer of 0.327 mm aluminium) was used and the images were obtained for stacks of PMMA sheets of nominal total thickness of 20, 40, 60 and 70 mm. The actual thickness of each stack was determined and used for the calculations. The value of the mAs for each exposure was adjusted to give a pixel value of ~500. For each image, the average pixel value and its variance were estimated over a fixed area of interest using the raw image data. Previously established linearity of the equipment was then used to scale both the pixel values and the variance to the values for 100 mAs. The SNR at 100 mAs was then taken as the scaled pixel value divided by the scaled standard deviation.

The calculated and measured results for both the pixel value and the SNR were normalised for the purposes of comparison. For the pixel value, both sets of results were normalised to a value of 1 for 20 mm of PMMA. For the SNR, both sets of results were normalised by the measured value of the SNR for 20 mm of PMMA sheet.

As the thickness of the material between the bottom of the breast and the image receptor and the thickness of the CsI detector were not known, in fact, the comparison was a fitting process to explore possible values of the detector thickness and the breast support/detector entrance material. In this respect, it is noted that a further check of the program has been made by simulating the Lausanne mammography phantom and comparing the measurements with the calculations of image properties[5].

RESULTS

Calibration of the Monte Carlo simulation against experiment

The process of fitting the measured and calculated pixels and SNR values by adjusting the thickness of the CsI phosphor and the carbon fibre composite breast support (simulating all material between the bottom of the breast and the phosphor apart from the anti-scatter grid) proved not to be very sensitive to the thickness of these two materials. The increase in one could be compensated by a decrease in the other to achieve a good fit. For the results presented here, the thickness of the phosphor and the breast support were considered to be 90 mg cm^{-2} and 4 mm, respectively.

Figure 2 shows the comparison of the normalised values of the measured and calculated pixel values for the four PMMA slabs at a fixed exposure. An excellent agreement is seen. The ratios of the pairs of values at the nominal thickness of 40, 60 and 70 mm are 1.016, 1.009 and 0.994, respectively, which

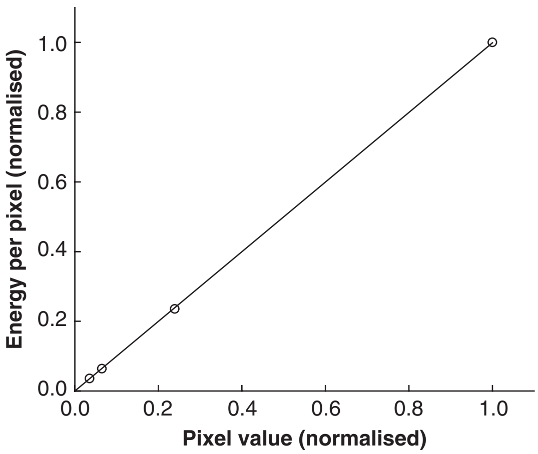

Figure 2. Comparison of calculated values of energy deposited per pixel for slab phantoms of PMMA using a Mo/Mo 28 kV spectrum and the experimental pixel values for the same case. Results in each case are normalised to a value of 1 for the 20 mm phantom.

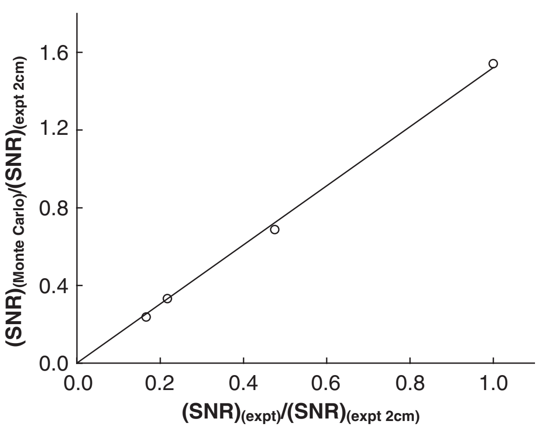

Figure 3. Comparison of calculated SNR values for slab phantoms of PMMA using a Mo/Mo 28 kV spectrum and the experimental values of SNR for the same exposure (80 mAs). Results are normalised to the experimental values for the 20 mm phantom.

demonstrates an excellent agreement over a pixel value range of 28:1.

Figure 3 shows the comparison of the normalised values of the measured and calculated SNR values for the four PMMA slabs at a fixed exposure. The points again lie on a straight line. The ratios of the pairs of values at the nominal thickness of 20, 40, 60 and 70 mm are 1.542, 1.446, 1.529 and 1.419, respectively. The mean and SD of these ratios are 1.484 and 0.06 (4%), respectively, which demonstrates a good agreement with SNR over a pixel value range of 28:1. The statistical error on the Monte Carlo estimate of SNR was ~0.5%. It should be noted that the equality of calculated and measured SNR is not expected because the computer model does not account for the spread of the point-spread function of the image receptor beyond one pixel. This provides some noise averaging and increases the measured SNR.

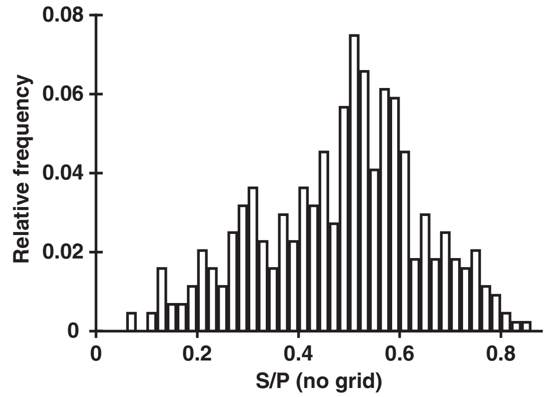

Figure 4. Histogram of the values of S/P ratio calculated without an anti-scatter grid.

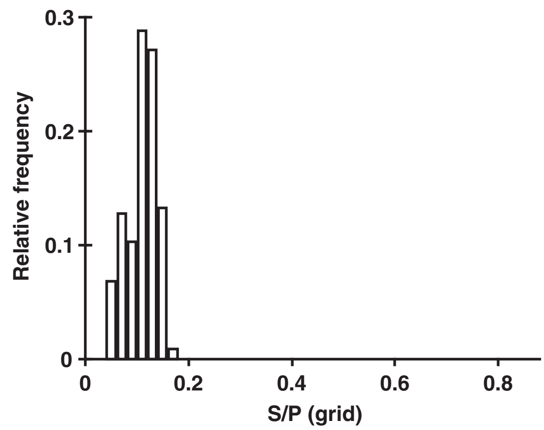

Figure 5. Histogram of the values of S/P ratio calculated with an anti-scatter grid. To facilitate comparison, the scale of the horizontal axis is the same as that in Figure 4.

Calculations with the voxel phantom

The S/P ratios with and without the mammographic anti-scatter grid have been computed for an array of 35 × 18 image points and the histograms of these quantities are shown in Figures 4 and 5 for the 50 mm breast phantom and a 28 kV Mo/Mo spectrum. The S/P ratios without the grid show significant variation

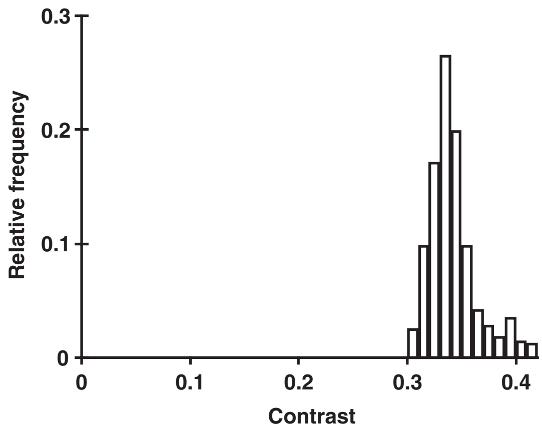

Figure 6. Histogram of the values of the contrast for a microcalcification. The calculation of this quantity neglects the receptor and geometrical unsharpness.

over the image reaching a maximum value of 0.82 in the dense region of the breast and showing a range in the magnitude of 8:1. This will produce important changes in the contrast of the image, which is proportional to $(1+\mathrm{S/P})^{-1}$. The variation of the S/P ratio across the image is of consequence for digital tomosynthesis, where the images are obtained without an anti-scatter grid. Figure 5 shows the S/P ratio obtained with a grid for the same situation. It reaches a maximum value of 0.14 with a range of values of 3:1. Although much smaller than the values obtained without the grid, the magnitude and variation of S/P ratio with the grid are still significant, influencing both contrast and the contrast-to-noise ratio.

The contrast for a given detail varies across the image due to changes in the S/P ratio and in beam hardening, with both effects operating in the same direction. Figure 6 shows the variation of the contrast for a 200 μm calcification as it is positioned in-line with different pixels in the image. The range of contrast variation is 1.33:1, arising from the variations in both beam hardening and S/P ratio. Significant variation in detectability with position can therefore be expected for small lesions.

CONCLUSIONS

A computer model of mammography incorporating a realistic breast simulation has been developed, which has significant advantages over the models using homogenous phantoms. Calculations have demonstrated the power of the model for the study of image properties, showing important variation in the S/P ratio and contrast with position in the image. The model is of value for the simulation of conventional imaging and digital tomosynthesis.

ACKNOWLEDGEMENTS

We express our thanks to Elly Castellano who made the measurements on the GE 2000D digital mammographic unit. This work has been funded by the Commission of European Communities 5th Framework Programme (grant CT200-0036 9, the ‘Radius Project’) and the US Department of Defense (grant DAMD 17-98-1-1819).

REFERENCES

1. Dance, D. R., Hunt, R. A., Bakic, P. R., Maidment, A. D. A., Sandborg, M., Ullman, G. and Alm Carlsson, G. *Breast dosimetry using high-resolution voxel phantoms*. Radiat. Prot. Dosim. **114**(1-3), 359–363 (2005).
2. Dance, D. R., Skinner, C. L., Young, K. C., Beckett, J. R. and Kotre, C. J. *Additional factors for the estimation of mean glandular breast dose using the UK mammography dosimetry protocol*. Phys. Med. Biol. **45**, 3225–3240 (2000).
3. Dance, D. R., Thilander Klang, A., Sandborg, M., Skinner, C. L., Castellano Smith, I. A. and Alm Carlsson, G. *Influence of anode/filter material and tube potential on contrast, signal-to-noise ratio and average absorbed dose in mammography: a Monte Carlo study*. Br. J. Radiol. **73**, 1056–1067 (2000).
4. Bakic, P. R., Albert, M., Brzakovic, D. and Maidment, A. D. A. *Mammogram synthesis using a 3D simulation. 1. Breast tissue model and image acquisition simulation*. Med. Phys. **29**, 2131–2139 (2002).
5. Hunt, R. A., Dance, D. R., Pachoud, M., Almcarlsson, G., Sandborg, M., Ullman, G and Verdon, F.R. Monte Carlo stimulation of a mammegraphic test object. Radiat. Prot. Dosim. **114**(1-3), 432–435 (2005).